Biosensors and Bioelectronics 294 (2026) 118217

Contents lists available at ScienceDirect

Biosensors and Bioelectronics

journal homepage: www.elsevier.com/locate/bios

A molecular finger-imprinting approach for detecting dental enamel amelogenins via surface plasmon resonance and bio-layer interferometry

Valentina Camagni [a,b], Davide Sestaioni [c], Simone Ventisette [c], Lucrezia Gatti [b], Fabrice Bray [d], Christian Rolando [d], Tina Lüdecke [e], Giorgia Sciutto [b], Silvia Prati [b], Rocco Mazzeo [b], Simona Scarano [c,f,*]

[a] Department of Sciences of Antiquity, "La Sapienza" University of Rome, Rome, Italy
[b] Department of Chemistry "Giacomo Ciamician", University of Bologna, Ravenna Campus, Italy
[c] Department of Chemistry "Ugo Schiff', University of Florence, Sesto Fiorentino, Italy
[d] Miniaturisation pour la synthèse, l'analyse et la protéomique (MSAP), CNRS, Université de Lille, F-59000, Lille, France
[e] Emmy Noether Group for Hominin Meat Consumption, Max Planck Institute for Chemistry, Hahn-Meitner-Weg 1, Mainz, Germany
[f] National Interuniversity Consortium of Materials Science and Technology (INSTM), Florence, Italy

ARTICLE INFO

Keywords:
Amelogenins
Dental enamel proteins
Molecularly imprinted bio-polymers
Biosensors
Surface plasmon resonance
Bio-layer interferometry

ABSTRACT

Amelogenins (AMGs) are extracellular matrix proteins essential for enamel development. During this process, resident proteases cleave the full-length proteins into a heterogeneous mixture of peptides that is retained within mature enamel. Current enamel proteomics primarily focuses on detecting sexually dimorphic AMG peptides for sex identification in archaeological and forensic contexts. In parallel, AMG pattern analysis supports research into enamel-related pathologies and clinical applications. Furthermore, AMG expression in odontogenic epithelium is considered a potential indicator for the histological behavior of tumors. Although their detection is commonly achieved by mass spectrometry, no fast, low-cost, miniaturizable platforms with minimal sample preparation are currently available. To address the complexity of real enamel extracts, we developed synthetic receptors based on molecularly imprinted polynorepinephrine (MIPNE). We integrated them into Surface Plasmon Resonance (SPR) and Bio-Layer Interferometry (BLI) platforms. Leveraging the conventional Single-Epitope Imprinting (SEI) strategy, we introduced an original "Finger-Imprinting" (FI) approach that exploits the direct imprinting of human enamel extracts. SPR binding assays toward standard AMGX revealed superior affinity and capacity for FI-imprinted receptors ($K_D = 3.6 \times 10^{-8}$ M, $R_{max} = 2286 \pm 5$ RU) compared with SEI-imprinted counterparts ($K_D = 4.9 \times 10^{-7}$ M, $R_{max} = 157 \pm 6$ RU). BLI enabled the selective recognition of AMG-derived fragments in enamel extracts thanks to a higher representation of the binding cavities. We additionally achieved encouraging evidence of sex differentiation in real samples. This work introduces a novel imprinting concept that adapts the complexity of degraded/digested proteins in real samples to pattern analysis via biosensing.

1. Introduction

Amelogenins (AMGs) are proteins with a key role in dental enamel formation (amelogenesis), cellular differentiation, and tissue repair (Moradian-Oldak and George, 2021). AMG isoforms and splice variants represent 90 % of the total enamel protein content. During amelogenesis, full-length parent proteins are digested and mostly reabsorbed by resident proteases, which ensures complete enamel maturation (Rathsam et al., 2018). The AMGs primary amino acid (aa) sequence is highly conserved across species with the variations mainly observed in the length of the hydrophobic region. It is typically organized into three main regions: the tyrosine-rich amelogenin peptide (TRAP), the hydrophobic core (HR), and the C-terminal sequence (CTHR) (Fig. 1). The TRAP is preceded by a signal peptide (16 aa), which is removed by signal peptidase immediately after secretion (Shaw et al., 2020).

While extensive studies have focused on the structural role of AMGs,

This article is part of a special issue entitled: Biosensors 2025 published in Biosensors and Bioelectronics.

* Corresponding author. Department of Chemistry "Ugo Schiff', University of Florence, Sesto Fiorentino, Italy.
E-mail address: simona.scarano@unifi.it (S. Scarano).

https://doi.org/10.1016/j.bios.2025.118217
Received 31 July 2025; Received in revised form 20 October 2025; Accepted 11 November 2025
Available online 12 November 2025

evidence suggests that certain AMG gene splice products may participate in signal transduction during tooth development (Veis, 2003). Beyond their presence in the dental enamel matrix, studies have found these proteins in various other tissues (Deutsch et al., 2006; Gruenbaum-Cohen et al., 2009), as well as in connection with benign and malignant odontogenic tumors (Kumamoto et al., 2001; Crivelini et al., 2012; Zakaraia et al., 2018). The presence of specific mutations in AMG primary sequence has also been linked to inherited diseases and disorders affecting the hardness, color, size, and shape of teeth, such as *amelogenesis imperfecta* (Lagerström-Fermér and Landegren, 1995; Shemirani et al., 2023). In this framework, identification of AMGs as biomolecular markers could improve the speed and accuracy of diagnosis and treatment decisions, once suitable tests are developed. In humans, AMG-encoding genes are located on the X and Y chromosomes. Consequently, the derived sex-specific isoforms are also utilized in forensic and archaeological investigations for sex attribution of skeletal remains (Cintas-Peña et al., 2023; Lopes Cardoso et al., 2024). AMGs are typically identified by Mass Spectrometry (MS) (Stewart et al., 2017), but this approach has not yet been translated into fast, low-cost platforms that allow miniaturization, long shelf-life, and minimal sample preparation. In this framework, we propose the use of biosensors coupled with next-generation bioinspired receptors based on molecularly imprinted soft polymers derived from endogenous neurotransmitters, such as polynorepinephrine (PNE). Molecularly imprinted PNE (MIPNE) have recently demonstrated their practical use as antibody alternatives in affinity-based optical sensing (Baldoneschi et al., 2020; Torrini et al., 2022b, 2024; Sestaioni et al., 2024; Ventisette et al., 2025) and bioanalytical assays (Torrini et al., 2022a, 2023; Battaglia et al., 2023), offering broader selectivity and higher robustness (Bhakta and Mishra, 2021; Milanković et al., 2024). Their preparation relies on a low-cost, one-step protocol performed in water at room temperature within a few hours, co-polymerizing the NE monomer and a short synthetic peptide (epitope) in bulk. By the SEI approach, an epitope sequence is rationally designed *in silico* from the target protein, enabling in-house development and theoretical adaptability to virtually any protein biomarker. As demonstrated in our previous studies (Baldoneschi et al., 2020; Sestaioni et al., 2024; Ventisette et al., 2025), MIPNE nanofilms exhibit homogeneous nanometric coatings and stable surface chemistry.

In fact, one of the key advantages of PNE is its ability to spontaneously deposit as a nanometric film onto virtually any substrate — including metals, glass and polymers — during polymerization. This feature enables the fast and low-cost fabrication of MIPNE coatings in a fully customizable manner, without the need for primers or surface activation. Notably, the synthesis is intrinsically green, taking place in aqueous medium and at room temperature without organic solvents. After polymerization, the epitope is removed by washing, leaving behind stable and selective 3D cavities that are structurally complementary to the imprint. These binding sites enable the reversible and specific recognition of the full-length target protein. The MIPNE films withstand multiple usage and long-term storage (months to years) without significant loss of activity. When needed, the polymer layer can be removed, enabling complete regeneration of the original support (Sestaioni et al., 2024). Recent studies have attempted to move beyond the SEI strategy by imprinting multiple peptides or protein mixtures to enhance surface avidity (Wang et al., 2023). However, none of these approaches rely on PNE chemistry, and direct imprinting of an entire protein extract from a real, complex biological matrix has — to our knowledge — never been reported. Applying this strategy to enamel AMGs offers a compelling pathway towards both personalized diagnostics and sex determination workflows.

In this work, we present the design and development of original MIPNE as biomimetic receptors capable of binding full-length AMGs, both from standard solutions and protein extracts of human enamel. Taking the SEI approach as the reference imprinting strategy, we introduce an original "Finger-Imprinting" (FI) method, which involves the direct imprinting of the entire enamel protein extract instead of a single etopipe. This strategy aims to increase the representation of AMG-derived fragments on the MIPNE surface naturally present in enamel through their collective imprinting at the receptor surface. By amplifying the "signature" of the recognition cavities, the receptor is expected to achieve an enhanced differential response — potentially allowing fine discrimination between closely related variants, even at low abundance. To our knowledge, this represents the first attempt to capture complex protein patterns via direct molecular imprinting, opening new perspectives for the analysis of proteins that have undergone enzymatic and/or environmental degradation.

The case study of AMGs is particularly well suited for this methodological advancement with MIPNE, due to the complex and variable presentation of AMG fragments in mature enamel extracts. The rationale behind this approach stems from recent findings demonstrating that PNE preferentially imprints peptide sequences characterized by specific combinations of net charge, isoelectric point, hydrophobicity and aromatic residues (Sestaioni et al., 2025). These descriptors modulate the strength of hydrogen bonding, electrostatic interactions and π–π stacking occurring during polymerization, ultimately dictating both the quality of the imprinted cavity and the affinity toward the full-length protein. Such intrinsic selectivity provides a solid foundation for extending imprinting from rationally designed epitopes to complex protein mixtures. Surface Plasmon Resonance (SPR) was employed as the reference platform for the foundational development and

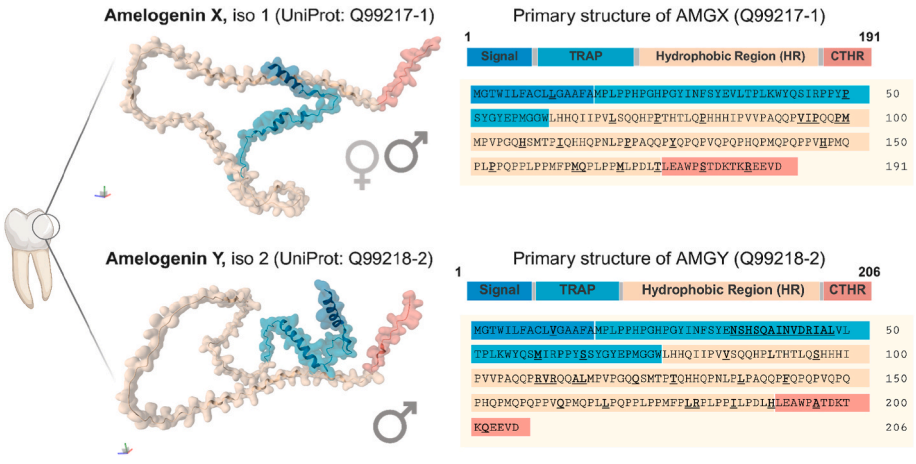

Fig. 1. AMGs structures and aa sequences with cartoon representation of the regions. The aa sequences indicated are the canonical isoforms reported in UniProt. Created by BioRender. Camagni, V. (2025). https://BioRender.com/p88c977.

optimization of the detection strategy. To complement this, Bio-Layer Interferometry (BLI) was used to increase throughput on real samples, reduce sample volume requirements (4 μL per assay), and provide signals unaffected by matrix refractive index. Together, these two label-free, real-time techniques enabled affinity measurements, binding constant determination, and high-throughput screening. Additionally, the data generated were suitable for highly informative two-dimensional visualizations and interpretation through the t-Distributed Stochastic Neighbor Embedding (t-SNE) analysis.

2. Materials and methods

2.1. Reagents and buffers

All chemical and reagents were of analytical grade and purchased from Merck KGaA (Darmstadt, Germany), unless otherwise specified. These included L-norepinephrine hydrochloride (NE, ≧ 98.0 %), tris (hydroxymethyl) aminomethane hydrochloride (Tris-HCl, ≧ 99.0 %), 4-(2-Hydroxyethyl) piperazine-1-ethanesulfonic acid (HEPES), potassium chloride, sodium chloride, sodium phosphate monobasic monohydrate, sodium phosphate dibasic, hydrochloric acid, acetic acid (≧ 99.7 %), sodium dodecyl sulfate (SDS), polyoxyethylene sorbitan monooleate (Tween-20), 11-mercapto-1-decanol (97 %), 6-mercapto-1-hexanol (97 %), and recombinant human amelogenin isoform X (expressed in *E. coli*, cat.: SAE0117, acronym AMGX). All custom peptides were supplied by GenScript (Leiden, Netherlands). These included P162_L9 (^{162}AWPSTDKTK^{170}, MW = 1033.15 g mol^{-1}), HSAr (^{558}EVENDEMP^{565}, MW = 962.00 g mol^{-1}), and P19 (^{19}NSHSQA^{24}, MW = 642.63 g mol^{-1}). Ultrapure Milli-Q™ water (R ≧ 18.2 MΩ cm) was used to prepare all the buffer solutions. HBS-EP (10.00 mM HEPES, 150 mM NaCl, 3 mM EDTA, 0.005 % Tween-20, pH 7.4) and PBS (140.00 mM NaCl, 2.68 mM KCl, 3.56 mM NaH2PO4, 6.44 mM Na2HPO4, pH 7.4), both filtered through a 0.22 μm Millipore filter, were used as dilution and binding buffers for all SPR experiments.

2.2. Dental samples

Seventeen permanent teeth from 14 individuals (Table S1), originally extracted for clinical reasons (e.g., orthodontic or pathological conditions) and otherwise destined for disposal, were voluntarily donated to the Max Planck Institute for Chemistry (Germany). Written informed consent forms were signed by each donor, explicitly authorizing their use for scientific research. Samples were fully anonymized at the time of collection, with no clinical data recorded or analyzed. The study was conducted in accordance with the World Medical Association's Declaration of Helsinki. Given the complete anonymization and the surgical-waste nature of the material, no additional ethical approval was required under current national regulations.

2.3. Instrumentation

SPR measurements were carried out using Biacore X100 on bare gold sensor chips (Cytiva Sweden AB, Uppsala). BLI measurements were executed by Octet N1® on optical fiber tips Octet APS® (Sartorius AG, Goettingen, Germany). Liquid chromatography−mass spectrometry/mass spectrometry (LC−MS/MS) analyses were performed by a Mass spectrometer Orbitrap Q Exactive plus coupled to HPLC microfluidic system U3000 RSLC (ThermoFisher Scientific, Waltham, Massachusetts, USA), following the published protocol with minor modifications, excluding trypsin digestion (Bray et al., 2023). LC-MS/MS data were processed via database search using the software PEAKS X+ (PEAKS Studio, Bioinformatics Solutions Inc, Canada). Samples were analyzed at least three times to infer Standard Deviation (SD) and Relative Standard Deviation (RSD).

2.4. Protein extraction protocol from enamel samples

To prepare enamel for protein extraction, each tooth was drilled using a handheld drill equipped with a 0.9 mm diamond head tip, operated at low to medium speed (<2500 rpm) to collect enamel powder. From each tooth, 1 ± 0.1 mg of enamel powder was weighted in Eppendorf Protein LoBind tubes in triplicate. Protein extraction was carried out via acid demineralization at pH 1.00 in 150.0 μL 0.10 M HCl per sample to reach the complete dissolution of the mineral matrix. The extract was then sonicated at 100 % amplitude for 10 min. Inorganic components were precipitated by adjusting the pH to 12.00 through the addition of 187.5 μL of 0.10 M NaOH for each sample. Following centrifugation at 13,500 rpm for 10 min, the supernatant was collected and the pH was neutralized with HCl.

2.5. Preparation of MIPNE receptors on SPR gold chips

MIPNE receptors were directly synthesized on bare gold SPR sensor chips. When the SEI approach was applied, the P162_L9 epitope was used as the imprinting template. A 150 μL polymerization solution containing the functional monomer (NE, 2.00 g L^{-1}/9.72 mmol L^{-1} in 10.00 mmol L^{-1} Tris-HCl, pH 8.50) and the template (413.26 μg mL^{-1}/400.00 μmol L^{-1}) was deposited onto each chip by drop-casting. MIPNE nanofilms were then grown at 25.0 ± 0.5 °C in a thermostatic oven for 5 h as previously reported (Torrini et al., 2022b). FI-PNE were prepared by direct drop casting the enamel extract onto the bare gold chip. The polymerization solution consisted of the functional monomer (NE, 1.00 g L^{-1} (4.86 mmol L^{-1}) in 10.00 mmol L^{-1} Tris-HCl pH 8.50) and the extract (50 % v/v), and the subsequent steps followed the same protocol as for the P162_L9 epitope. All the MIPNE receptors were finally passivated and activated to remove the imprinted template(s) before analysis as elsewhere reported (Sestaioni et al., 2024).

2.6. SPR measurements

MIPNE obtained by the SEI approach were evaluated by Single Cycle Kinetic (SCK) analysis towards both the peptide template (25.00–200.00 μmol L^{-1} in PBS pH 7.40) and the AMGX protein (0.10–1.00 μmol L^{-1} in HBS-EP pH 7.40), by following a protocol previously reported (Torrini et al., 2022b; Sestaioni et al., 2024). Three measuring cycles were performed for each SCK analysis, regenerating the surface after each cycle. Regeneration steps were: one 24-s injection of 10.00 mmol L^{-1} HCl after each peptide measurement cycle, and two 24-s serial injections of 10.00 mmol L^{-1} HCl followed by a single 24-s injection of SDS (0.05 % v/v) after AMGX measurements. Kinetic and affinity parameters (k_a, k_d, K_D, R_{max}, Chi^2) were inferred by applying the two-state reaction model and the 1:1 Langmuir binding model to the data related to the peptide and the protein testing, respectively, using the BIAEvaluation 3.1 Software (Cytiva Sweden AB, Uppsala) (Karlsson and Fält, 1997; Torrini et al., 2022b; Sestaioni et al., 2024). HSAr, a peptide designed on the sequence of human serum albumin (HSA, UniProt code: P02768), was selected as a negative control and tested at 200.00 μmol L^{-1}. HSA was chosen as it has been previously reported as a component of dental enamel extracts (Castiblanco et al., 2015). The binding behavior of the receptors was not evaluated towards the AMGY protein due to the absence of the commercially available full-length AMGY protein or appropriate purified standards covering the complete aa sequence. At the time of experimentation, only partial AMGY sequences lacking the critical C-terminal region were accessible, rendering them unsuitable for a comprehensive assessment of the MIPNE recognition capabilities.

2.7. Preparation of MIPNE receptors on BLI optical fibers

MIPNE receptors were prepared by following the SEI approach on Octet APS® sensors using the NE monomer and P162_L9 peptide

template used for SPR experiments. APS® sensors consist of optical fiber tips modified to expose amino-propyl silane (APS) moieties, allowing amino coupling conjugation in classical immuno-based assays. MIPNE receptors were fabricated on APS® tips by directly immersing them in a polymerization solution containing the functional monomer (NE, 1.00 g L^{-1}; 4.86 mmol L^{-1} in 10.00 mmol L^{-1} Tris-HCl, pH 8.5) and the template (2.07 μg mL^{-1}; 2.00 μmol L^{-1}), following a recently reported procedure (Ventisette et al., 2025). FI-PNE receptors were synthesized on APS® tips by immersion in a polymerization solution consisting of the functional monomer (NE, 1.00 g L^{-1} (4.86 mmol L^{-1}) in 10.00 mmol L^{-1} Tris-HCl pH 8.5) and enamel extract (50 % v/v), following the aforementioned protocol.

2.8. BLI measurements

Each analyte was tested in triplicate after having recorded 60 s of baseline signal with the binding buffer (HBS-EP pH 7.4). 4.00 μL of samples were deposited on the sample holder and 120 s of association were recorded. On SEI-PNE tips, the peptide P162_L9 and the AMGX protein were used as positive controls at 200.00 μmol L^{-1} and 0.01 μmol L^{-1}, respectively. HSAr and P19 were included as negative controls at 200.00 μmol L^{-1}. On FI-PNE tips, imprinted with either male or female extracts, the same positive and negative references were tested. However, P19 cannot be considered a negative control for male-imprinted tips. Nevertheless, given the very low AMGY-to-AMGX ratio in enamel, only a negligible signal would be expected. Protein extracts were tested without any additional processing. HBS-EP was used both as a dilution and binding buffer. After the association, a dissociation time of 120 s in HBS-EP was applied, and the sensor surface was then regenerated with two consecutive washings of 10 mM HCl (60 s) and SDS (0.005 % v/v, 60 s). Kinetic and affinity parameters (k_a, k_d, K_D, R_{max}, R_{eq}) were established by applying the 1:1 Langmuir binding model to the experimental data using the Octet® N1 1.4.0.13 Software (Sartorius AG, Gottingen, Germany) (Ventisette et al., 2025).

2.9. BLI data analysis by unsupervised machine learning methods

Sensorgrams and binding data obtained by BLI were handled through t-Distributed Stochastic Neighbor Embedding (t-SNE) analysis by using Orange Data Mining 3.38.1 Software (Orange Data Mining) (Demšar et al., 2013). t-SNE is a non-linear dimensionality reduction technique, able to generate lower-dimensional representations of high-dimensional data while preserving their underlying structure, enabling intuitive 2D visualizations and revealing latent clustering patterns according to the relative similarities among objects (data). To assess performance, hyperparameters were tuned and the proper combinations were perplexity = 5 and exaggeration = 1.5. The input dataset included experimental data from BLI measurements carried out on tips modified with MIPNE via SEI with the P162_L9 peptide (2 tips, AmelXY_1, AmelXY_2), FI-PNE with female extracts (3 tips, 04F, 05F, 15F), and male extracts (3 tips, 06M, 08M, 16M). Numerical features included all experimental BLI signals sampled at several injection time points (180 s, 200 s, 250 s, 300 s), signal ratios (200 s/300 s, 250 s/300 s), signal differences (200 s–180 s, 250 s–180 s, 300 s–180 s), R_{max}, and R_{eq}. No target was set. t-SNE preprocessing included Z-score normalization of data. All the other information included in the dataset (analyte type, Sample ID, sex analyte etc.) were set as text meta.

3. Results

3.1. Epitope selection for AMGs PNE imprinting

The canonical forms of AMGX (UniProt code: Q99217-1, 191 residues, https://www.uniprot.org/uniprotkb/Q99217/entry) and AMGY (UniProt code: Q99218-2, 206 residues, https://www.uniprot.org/uniprotkb/Q99218/entry) were used as references for the SEI approach. A short synthetic peptide was designed on the whole sequences to develop the SEI-PNE receptor. Nevertheless, alternative splicing generates several variants of AMG transcripts, ultimately affecting the expression and functional diversification of proteins during odontogenesis (Veis, 2003; Iacob and Veis, 2006; Wang et al., 2013). Three splice variants have been identified for AMGX (Q99217-1, Q99217-2, Q99217-3) and two for AMGY (Q99218-1, Q99218-2) (Fig. S1). The expression of AMGX and AMGY is also reported to be quantitatively different, with about 90 % of all RNA transcripts expressed from the X chromosome and the rest from the Y chromosome (Chen et al., 1998; Bansal et al., 2012). Given the enzymatic cleavage of AMGs during enamel maturation, a preliminary mass spectrometry analysis was conducted on 17 contemporary tooth samples to identify the most represented protein fragments (Table S1). Undigested extracts revealed peptides with *m/z* 300–1500, including non-tryptic fragments mainly from AMGX (in all samples) and AMGY (in male samples), particularly within the hydrophilic TRAP and CTHR regions (Table S2, Fig. S2A–Q), together with other extracellular matrix proteins (Table S3). These findings guided epitope selection to ensure that the MIPNE could recognize both full-length AMGX and peptide fragments from real samples. To this aim, an in-house Python script was used, in which the AMGX sequence (Q99127-1) was the input information to create a library of peptide sequences ranging from 8 to 12 aa, obtaining 829 peptides (Fig. S3). In a second step, the library was ranked based on suitable physico-chemical peptide descriptors (Sestaioni et al., 2025). The output library included 12 candidate peptides (Fig. S4), predominantly located in the C-terminal hydrophilic region of AMGX (from residue 161 onward). Since LC-MS/MS analyses revealed the presence of peptides from this region in all female and male samples (Fig. S5), it was identified as the primary region of interest for the final selection. To ensure that the selected epitope could bind both the AMGX and AMGY forms, all splice variants were aligned to identify a region within the most conserved amino acid sequence (Fig. S6). To minimize non-specific interactions with other components of the dental enamel matrix, a preliminary BLAST analysis against the most abundant proteins identified in dental enamel studies was also performed (Fig. S7A–E). The final peptide selected was the n. 7, P162_L9 (^{162}AWPSTDKTK^{170}), which fully matched all three Q99127 splice products and exhibited 89 % homology with the two Q99128 splice products, differing only by a single S/A variation at the 165th aa (AWPATDKTK). It confirmed that the selected epitope is unique to AMG splice variants, except for a single amino acid S/A substitution (^{193}AWP<u>A</u>TDKTK^{201}, notation relative to AMGY, Uniprot ID: Q99218-2). Additionally, considering the relative abundance of mature human enamel proteins, AMGs account for nearly 90 % of the total protein content. Therefore, the matrix effect is not expected to significantly impact the results. This epitope was utilized to develop the related MIPNE by the SEI approach, as a positive reference for AMGX/Y binding.

3.2. Development of the SEI-PNE receptor by SPR

The SEI-PNE receptor was first characterized through SCK analyses by SPR testing the P162_L9 epitope as the analyte (Fig. 2A), following previously reported case studies (Torrini et al., 2022b; Sestaioni et al., 2025). The sensor was tested within the concentration range 25.00–200.00 μmol L^{-1}, giving $K_D = 4.9\ 10^{-7}$ M and $R_{max} = 157 \pm 6$ RU. Surface accumulation of the epitope was evaluated by plotting stability RU values against its concentration (Fig. 2B).

Considering the limited peptide length (9 aa), the sub-micromolar equilibrium dissociation constant obtained reflects high peptide/MIPNE affinity, ascribable to the favored peptide physical/chemical properties evaluated during the epitope selection step (Sestaioni et al., 2025). Thereafter, the full-length standard AMGX protein was tested within the concentration range 0.10–1.00 μmol L^{-1} (Fig. 2C–D). The range was chosen to reflect the supposed order of AMG concentration in real extract. In particular, knowing that AMGs correspond

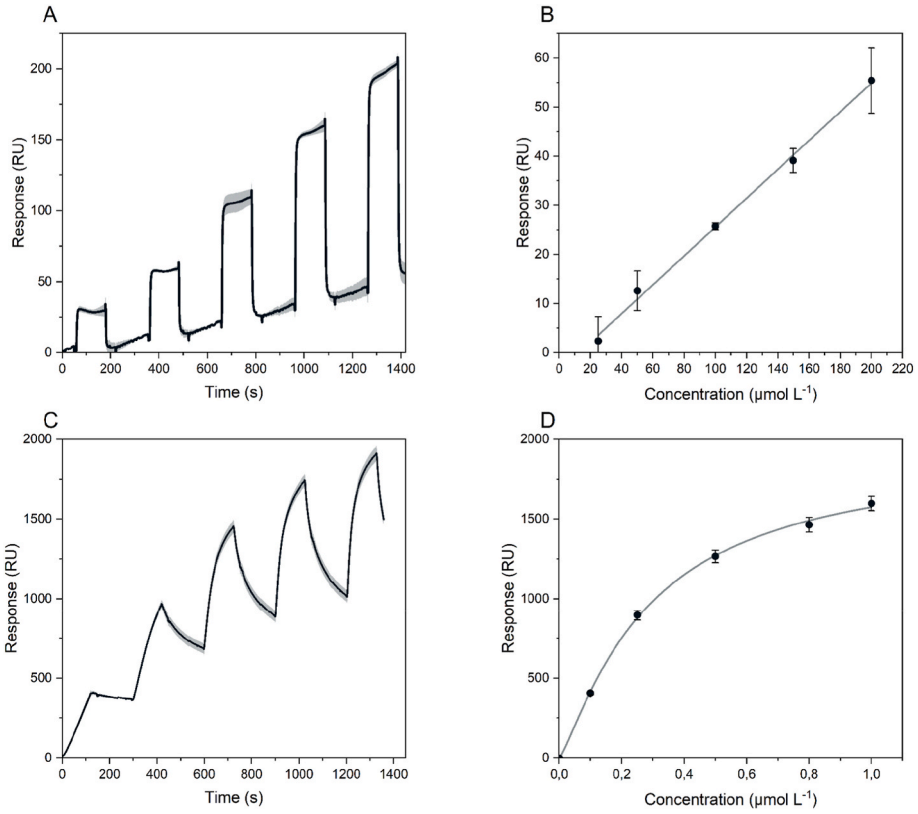

Fig. 2. Development of the SEI-PNE receptor by SPR. (A) SCK sensorgram testing the peptide template (P162_L9, 25.00–200.00 μmol L^{-1}) and, (B) RU values recorded at the end of each association phase; (C) SCK sensorgram testing the commercial protein (AMGX, 0.10–1.00 μmol L^{-1}) and, (D) RU values recorded after the end of the analyte injection, during the dissociation phase. Data represented as mean ± SD.

approximately to 0.9 % of the total mass of enamel, the AMGX content in our enamel extracts was approximated to 0.02 mg mL^{-1} (1.0 μmol L^{-1}), on the basis of the molecular weight of the full-length protein, which is 20 kDa. The affinity parameters obtained were $K_D = 7.34 \times 10^{-8}$ M and R_{max} = 1695 ± 4 RU, showing a marked improvement over the SEI approach. This trend was recurrent in our previous studies when shifting from short epitopes to whole protein binding to MIPNE. Likely, once the affinity complex is formed, the full protein can engage in additional weak local interactions that further stabilize the binding at the MIPNE surface. Consistently, the kinetic parameters, even if inferred by two fitting models, show faster association (k_a) and lower dissociation rates (k_d) for the protein compared to the epitope (Table S4). Since dissociation is concentration-independent, the reduced k_d may reflect more stable interactions within the binding cavities. Real enamel extracts were then tested on SEI-PNE without pre-treatment, yielding low but detectable signals, likely due to the low epitope fragment concentration (data not shown). Therefore, we developed a FI-PNE approach, imprinting the full enamel protein extract to better represent target fragments and enhance biosensor response.

3.3. Development of the FI-PNE approach

Preliminary tests were conducted to assess the feasibility of the FI-PNE approach. Given the 0.05 mol L^{-1} NaCl in the polymerization mix, we evaluated whether the increased ionic strength could affect PNE imprinting - an essential step for advancing the method. To simulate the extraction conditions, the P162_L9 epitope was used as an internal standard: instead of starting from enamel powder, an epitope solution was subjected to the full extraction protocol and then used as the imprinting template. This enabled us to evaluate the SEI-PNE strategy to assess the "imprint-ability" of a real extract under the final ionic conditions. The MIPNE obtained was tested against 10 nmol L^{-1} AMGX (Fig. S8), yielding binding values (66 ± 8 RU) comparable to those of the reference SEI-PNE, in which the epitope was not subjected to the simulated extraction procedure (59 ± 2 RU). This confirms that the enamel extraction solution does not affect the co-polymerization process. Moreover, polymerization was also carried out using 1.00 g L^{-1} PNE instead of 2.00 g L^{-1}, resulting in an improved binding signal of 111 ± 2 RU. These results suggest that thinner polymer layers favor binding of the full AMGX protein, likely due to the closer proximity of recognition sites to the plasmonic surface, where the evanescent field is strongest. Therefore, 1.00 g L^{-1} NE was selected for further method development.

3.4. Testing FI-PNE by SPR measurements

Based on the results obtained, a female enamel extract was selected based on LC-MS/MS results as a "high %coverage" sample (15F) for the direct imprinting of PNE on a bare gold SPR chip, obtaining the first FI-based reference receptor. The 15F extract was freshly prepared, imprinted, and tested by exploratory injections of P162_L9 to verify whether the CTHR region - on which P162_L9 was designed - is present in the whole enamel extract and able to be imprinted in PNE. As shown in Fig. 3A, the binding was effective and repeatable (26 ± 1 RU), although lower than the reference SEI-PNE receptor (56 ± 8 RU). Quantitative responses cannot be directly compared, as it is not possible to determine which and how many P162-containing peptides effectively generate binding cavities in the MIPNE. Nonetheless, the results confirm the presence of the sequence in the enamel extract and its affinity for NE. Both surfaces were also tested against AMGX and HSAr as positive and negative controls, respectively. The signal obtained with the standard AMGX protein was significantly higher than that of the SEI-PNE receptor, suggesting an enhanced binding capacity, likely due to the increased avidity conferred by imprinting the mixture of extract fragments. In

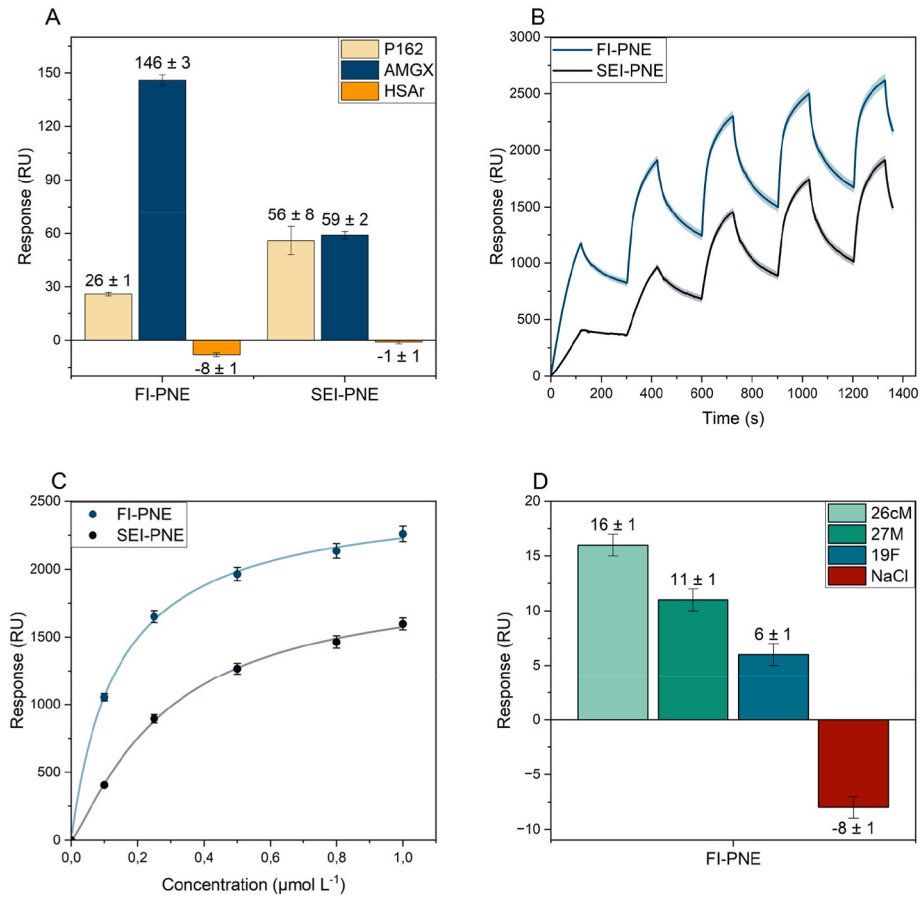

Fig. 3. Testing FI-PNE receptors by SPR measurements. (A) RU signals obtained on the FI-PNE and the SEI-PNE receptors for the P162_L9 epitope (200.00 μmol L^{-1}), the standard AMGX (10.00 nmol L^{-1}), and the negative control peptide (HSAr, 200.00 μmol L^{-1}); (B) SCK sensorgrams (n = 3) performed on both biosensors, testing the commercial protein (AMGX, concentration range 0.1–1.0 μmol L^{-1}); (C) RU values recorded after the end of the analyte injection, during the dissociation phase; (D) RU values for three different enamel extracts (26 cM, 27M, 19F) and a blank extract (0.1 mol L^{-1} NaCl). Data represented as mean ± SD.

contrast, the HSAr control peptide showed negligible binding (Fig. 3A).

The standard AMGX was then extensively tested by SCK analysis (Fig. 3B–C) to infer kinetic and affinity parameters ($K_D = 3.61\ 10^{-8}$ M, $R_{max} = 2286 \pm 5$ RU), which resulted in improvement with respect to the SEI-based receptor subjected to the same experimental conditions (Table S4). In fact, values for k_a and k_d were, respectively, $5.83 \times 10^4 \pm 3.40 \times 10^2$ s^{-1} M^{-1} and $2.10 \times 10^{-3} \pm 1.70 \times 10^{-5}$ s^{-1}. This demonstrates the successful imprinting of NE with components of the extract mostly related to AMG. Higher kinetics values could be the result of higher availability and representation of binding cavities, mimicking a polyclonal antibody binding.

These outcomes substantiated our progression to testing real enamel protein extracts as analytes. Therefore, untreated enamel extracts from two males and one female (26 cM, 27M, 19F) were preliminary investigated, giving valuable even if quite low binding signals (Fig. 3D). Despite promising results, higher throughput, lower sample consumption, and reduced buffer-related RI interference were needed for robust analysis of real enamel samples. BLI was therefore chosen as an alternative technique for further studies.

3.5. Application of FI-PNE to BLI biosensing

For BLI analyses, two SEI-PNE tips were first imprinted with peptide P162_L9 at a lower concentration (2.00 μmol L^{-1}) to mimic the expected AMG fragment levels in real samples. To check their functionality, the tips were tested with 10.00 nmol L^{-1} standard AMGX as a positive control, showing efficient binding (Fig. 4). To evaluate the selectivity, the SEI-PNE receptors were tested against the control peptides HSAr and P19. In particular, the P19 peptide was derived from the canonical AMGY sequence (UniProt ID: Q99218-1), selecting a region absent in AMGX to serve as a negative control. Both controls produced negligible signals, confirming the selective recognition of the SEI-PNE towards AMGX or its corresponding fragments.

Six FI-PNE tips were imprinted with enamel extracts from three female (04F, 05F, 15F) and three male individuals (06M, 08M, 16M). First, all tips were tested with 10.00 nmol L^{-1} standard AMGX and showed efficient binding (Fig. 4). This confirms that the FI-PNE surface carries specific binding cavities specifically imprinted by the AMG fragments extracted from enamel. The analysis of enamel protein extracts (F and M) also yielded significantly different signals compared to buffer (HBS-EP), blank controls (0.1 M NaCl), and the control peptides. The peptide P162_L9, tested at the same concentration (200.00 μmol L^{-1}), gave low but valuable binding signals partially distinguishable from both P19 and HSAr.

However, signal intensity alone is insufficient to fully characterize the complex recognition events inherent to these heterogeneous protein extracts. Consequently, the binding data were subjected to machine learning analysis to extract deeper insights from the observed profiles.

3.6. Machine learning analysis

t-SNE analysis of BLI data was performed to evidence the presence of specific binding signatures of AMGs from real extracts. Initially, binding data for P162_L9, AMGX, and HBS buffer were analyzed regardless of the imprinting method - *i.e.*, across all eight tips (three FI with male extracts, three FI with female extracts, and two SE with P162_L9) - resulting in

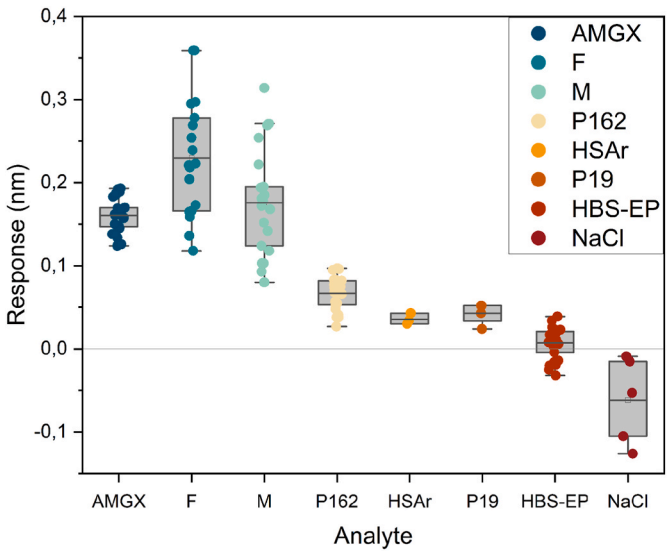

Fig. 4. Application of FI-PNE to BLI biosensing. Boxplot of the responses sampled after 200 s for the different SEI- and FI-PNE sensors tested against the peptide template (P162_L9, 200.00 μmol L^{-1}), standard protein (AMGX, 10.00 nmol L^{-1}) and enamel extracts (Table S1). Responses towards the analysis buffer (HBS-EP), blank extracts (0.1 mol L^{-1} NaCl), and negative control peptides (HSAr and P19, 200.00 μmol L^{-1}) are also reported. Data represented as response intensity values overlapped with boxplot (IQR: 25th to 75th percentile), the line inside the box indicates the median, and the whiskers extend to the minimum and maximum values.

three distinct groups (Fig. 5A). Notably, the AMGX group gathers all responses across donor-derived FI-PNE tips as well as SEI-PNE, indicating a consistent recognition profile despite enamel sample variability, including sex (F/M). This confirms that both reference targets, P162_L9 and standard AMGX, bind the SEI- and FI-PNE receptors with comparable behavior, yielding homogeneous responses that consistently cluster together.

Building on this, eight additional enamel extracts - four from female and four from male donors (Table S1) - were assayed as analytes. In this case, the same t-SNE analysis was performed on BLI data derived solely from interactions with the FI-PNE receptors, as shown in Fig. 5B. The responses from the enamel extracts (green) form a well-defined group, with some dispersion likely reflecting the natural variability of the samples. Nonetheless, they remain clearly distinguishable from the binding signal signatures of both P162_L9 and AMGX. To assess matrix effects, a 0.05 M NaCl solution was tested as a blank. The resulting signals formed a distinct cluster, confirming that enamel extract responses differ clearly from the blank and may reflect genuine binding. The inclusion of mixed enamel samples (MixF and MixM, *i.e.* equimolar mixtures of the three male and female extracts respectively) and negative controls (Blanks and NaCl) further validated the discriminative capacity of the system. Notably, MixF and MixM cluster within the individual enamel extracts, reflecting representative profiles and confirming the robustness of the FI-PNE receptors in recognizing a common enamel signature. Blanks (red) and NaCl (cyan) formed distinct clusters, clearly separated from enamel responses, confirming minimal non-specific binding to FI-PNE. The HSAr epitope (orange) is also grouped apart, reinforcing specificity. Finally, when highlighting the biological sex of the enamel donors, a partial spatial separation between male and female samples could be observed within the t-SNE projection (Fig. 6), suggesting that FI-PNE receptors might capture subtle, sex-related differences in the binding profiles. While preliminary, this result encourages future investigations involving a larger number of real samples to assess the potential of the method in discriminating enamel extracts on a biological basis.

4. Conclusion

In this work, we present a novel approach for imprinting biomimetic receptors using PNE to detect AMGs-derived fragments in human teeth, using a simple, rapid, and cost-effective protocol. A digestion-free extraction method was developed, requiring only 1 mg of enamel powder, with the entire extract directly used for imprinting, generating receptors tailored to the sample composition. The process is straightforward and uses biocompatible and biodegradable reagents. Binding interactions were evaluated through SPR and BLI, two real-time and label-free optical biosensing platforms. SPR provided a reference system, while BLI offered high throughput, low sample consumption, and compatibility with unpurified extracts. Together, they allowed in-depth assessment of imprinting efficiency and binding affinity. A direct comparison of binding performance between FI- and SEI-based receptors against standard AMGX revealed substantial improvement for the FI. The FI-PNE displayed affinity parameters ($K_D = 3.6 \times 10^{-8}$ M) that were over tenfold higher than the SEI receptors ($K_D = 4.9 \times 10^{-7}$ M). Crucially, the FI receptor also showed a vastly superior binding capacity ($R_{max} = 2286 \pm 5$ RU) compared to SEI ($R_{max} = 157 \pm 6$ RU). Subsequent evaluation of the FI-PNE with human enamel extracts using BLI confirmed its high selectivity. This enhanced recognition of AMG-derived fragments stems from the FI approach, which creates a more representative and effective ensemble of binding cavities. This FI strategy addresses the limitations of the conventional SEI approach when working with complex matrices like dental enamel and could offer a viable alternative to help overcome availability problems of full-length standard proteins in future applications. The results demonstrate the potential of MIBPs as stable, customizable alternatives to antibodies for rapid assays. Further optimization is needed to reinforce the method in distinguishing AMGX and AMGY isoforms, which could enhance applications in sex determination for forensic and archaeological studies. Finally, transitioning to a high-throughput format will expand the platform's practical use in both clinical and archaeological settings.

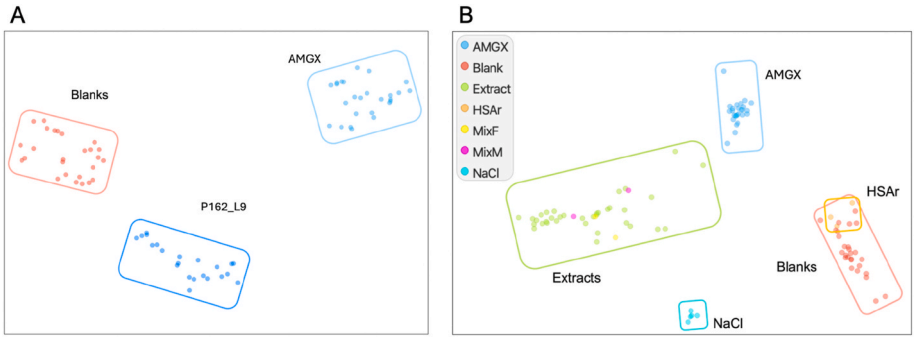

Fig. 5. t-SNE 2D projection of BLI responses obtained using: (A) the SEI-PNE (imprinted with P162_L9) and FI-PNE (imprinted with enamel extracts from male and female donors), (B) the FI-PNE strategy tested on male and female sample extracts. Data were pre-processed by normalization; perplexity = 5, exaggeration = 1.50.

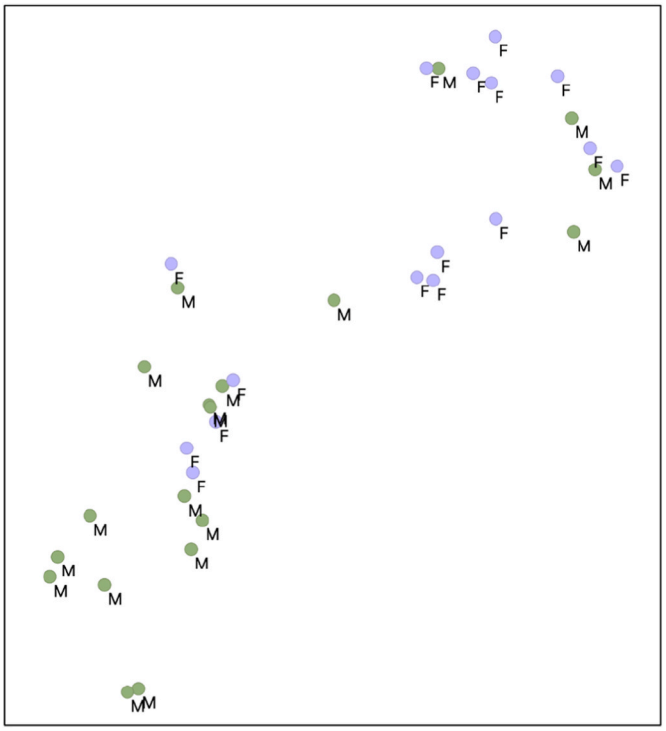

Fig. 6. 2D t-SNE projection of BLI responses obtained using the FI-PNE strategy, showing results from male (M) and female (F) sample extracts and highlighting a partial separation between sexes. Data were pre-processed by normalization; perplexity = 5, exaggeration = 1.5.

CRediT authorship contribution statement

Valentina Camagni: Writing – review & editing, Writing – original draft, Visualization, Methodology, Investigation, Formal analysis, Data curation, Conceptualization. **Davide Sestaioni:** Supervision, Investigation, Data curation. **Simone Ventisette:** Supervision, Investigation, Data curation. **Lucrezia Gatti:** Writing – review & editing, Methodology, Conceptualization. **Fabrice Bray:** Supervision, Resources, Methodology. **Christian Rolando:** Supervision, Resources, Methodology. **Tina Lüdecke:** Writing – review & editing, Resources. **Giorgia Sciutto:** Writing – review & editing, Supervision, Project administration, Methodology, Data curation, Conceptualization. **Silvia Prati:** Writing – review & editing, Supervision, Project administration, Methodology, Data curation, Conceptualization. **Rocco Mazzeo:** Writing – review & editing, Supervision, Project administration, Conceptualization. **Simona Scarano:** Writing – review & editing, Writing – original draft, Visualization, Validation, Supervision, Resources, Project administration, Methodology, Investigation, Funding acquisition, Formal analysis, Data curation, Conceptualization.

Declaration of generative AI and AI-assisted technologies in the writing process

During the preparation of this work, the author(s) used ChatGPT (2025 Version, OpenAI) in order to improve text readability, as well as checking grammar and spelling. After using this tool or service, the author(s) reviewed and edited the content as needed and take(s) full responsibility for the content of the publication.

Declaration of competing interest

The authors declare that they have no conflict of interest.

Acknowledgements

We acknowledge the support of the European Union by the Next Generation EU for the projects: PRIN PNRR 2022 Acr. SEROTONIN (P20227PWE5); Mission 4, Component 2, Inv. 1.5 (CUP B83C22003920001, Spoke 4), and Component 1 (CUP B53C22007250006, Spoke 5) of PE5 - Changes. The authors acknowledge MUR-, Dipartimenti di Eccellenza 2023–2027 (DICUS 2.0) to the Department of Chemistry "Ugo Schiff" of the University of Florence for partially funding Biacore X100 instrumentation with the project "Surface Plasmon Resonance (SPR) for chemical research: broad-spectrum applications, SPR Instrumentation Acquisition". T.L. acknowledges support from the Deutsche Forschungsgemeinschaft (DFG) through an Emmy Noether Fellowship (LU 2199/2-1). The authors acknowledge INSTM for hospitality and access to offices, resources and specific operational and scientific facilities.

Appendix A. Supplementary data

Supplementary data to this article can be found online at https://doi.org/10.1016/j.bios.2025.118217.

Data availability

Data will be made available on request.

References

Baldoneschi, V., Palladino, P., Banchini, M., Minunni, M., Scarano, S., 2020. Norepinephrine as new functional monomer for molecular imprinting: an applicative study for the optical sensing of cardiac biomarkers. Biosens. Bioelectron. 157. https://doi.org/10.1016/j.bios.2020.112161.

Bansal, A.K., Shetty, D.C., Bindal, R., Pathak, A., 2012. Amelogenin: a novel protein with diverse applications in genetic and molecular profiling. J. Oral Maxillofac. Pathol. 16 (3), 395–399. https://doi.org/10.4103/0973-029X.102495.

Battaglia, F., Bonelli, F., Sgorbini, M., Intorre, L., Minunni, M., Scarano, S., Meucci, V., 2023. Molecularly imprinted polymers as effective capturing receptors in a pseudo-ELISA immunoassay for procalcitonin detection in veterinary species. Anal. Methods 15 (1), 27–35. https://doi.org/10.1039/D2AY01175A.

Bhakta, S., Mishra, P., 2021. Molecularly imprinted polymer-based sensors for cancer biomarker detection. Sens. Acutators Rep. 3. https://doi.org/10.1016/j.snr.2021.100061.

Bray, F., Fabrizi, I., Flament, S., Locht, J.L., Antoine, P., Auguste, P., Rolando, C., 2023. Robust high-throughput proteomics identification and deamidation quantitation of extinct species up to Pleistocene with ultrahigh-resolution MALDI-FTICR mass spectrometry. Anal. Chem. https://doi.org/10.1021/acs.analchem.2c03301.

Castiblanco, G.A., Rutishauser, D., Ilag, L.L., Martignon, S., Castellanos, J.E., Mejía, W., 2015. Identification of proteins from human permanent erupted enamel. Eur. J. Oral Sci. 123 (6), 390–395.

Chen, E., Yuan, Z.A., Collier, P.M., Greene, S.R., Abrams, W.R., Gibson, C.W., 1998. Comparison of upstream regions of X-and Y-chromosomal amelogenin genes. https://doi.org/10.1016/S0378-1119(98)00300-X.

Cintas-Peña, M., Luciañez-Triviño, M., Montero Artús, R., Bileck, A., Bortel, P., Kanz, F., Rebay-Salisbury, K., García Sanjuán, L., 2023. Amelogenin peptide analyses reveal female leadership in copper Age Iberia (c. 2900–2650 BC). Sci. Rep. 13 (1), 9594. https://doi.org/10.1038/s41598-023-36368-x.

Crivelini, M.M., Felipini, R.C., Miyahara, G.I., de Sousa, S.C.O.M., 2012. Expression of odontogenic ameloblast-associated protein, amelotin, ameloblastin, and amelogenin in odontogenic tumors: immunohistochemical analysis and pathogenetic considerations. J. Oral Pathol. Med. 41, 272–280. https://doi.org/10.1111/j.1600-0714.2011.01079.x.

Demšar, J., Erjavec, A., Hočevar, T., Milutinovič, M., Možina, M., Toplak, M., Umek, L., Zbontar, J., Zupan, B., 2013. Orange: data mining toolbox in python. J. Mach. Learn. Res. 14, 2349–2353.

Deutsch, D., Haze-Filderman, A., Blumenfeld, A., Dafni, L., Leiser, Y., Shay, B., Gruenbaum-Cohen, Y., Rosenfeld, E., Fermon, E., Zimmermann, B., Haegewald, S., Bernimoulin, J.-P., Taylor, A.L., 2006. Amelogenin, a major structural protein in mineralizing enamel, is also expressed in soft tissues: brain and cells of the hematopoietic system. Eur. J. Oral Sci. 114, 183–189. https://doi.org/10.1111/j.1600-0722.2006.00301.x.

Gruenbaum-Cohen, Y., Tucker, A.S., Haze, A., Shilo, D., Taylor, A.L., Shay, B., Sharpe, P. T., Mitsiadis, T.A., Ornoy, A., Blumenfeld, A., Deutsch, D., 2009. Amelogenin in cranio-facial development: the tooth as a model to study the role of amelogenin during embryogenesis. J. Exp. Zool. B Mol. Dev. Evol. 312 (5), 445–457. https://doi.org/10.1002/jez.b.21255.

Iacob, S., Veis, A., 2006. Identification of temporal and spatial expression patterns of amelogenin isoforms during mouse molar development. Eur. J. Oral Sci. 194–200. https://doi.org/10.1111/j.1600-0722.2006.00287.x.

Karlsson, R., Fält, A., 1997. Experimental design for kinetic analysis of protein-protein interactions with surface plasmon resonance biosensors. J. Immunol. Methods 200 (1–2), 121–133. https://doi.org/10.1016/S0022-1759(96)00195-0.

Kumamoto, H., Yoshida, M., Ooya, K., 2001. Immunohistochemical detection of amelogenin and cytokeratin 19 in epithelial odontogenic tumors. Oral Dis. 7 (3), 171–176. https://doi.org/10.1034/j.1601-0825.2001.70306.x.

Lagerström-Fermér, M., Landegren, U., 1995. Understanding enamel Formation from mutations causing X-Linked amelogenesis imperfecta. Connect. Tissue Res. 32 (1–4), 241–246. https://doi.org/10.3109/03008209509013729.

Lopes Cardoso, I., Moreira, M.T., Dupuis, C., Castro, F., Guimarães, M.I., 2024. Amelogenin-based molecular methods for sexual dimorphism identification: protocol of a scoping review. Forensic Sci. 4 (4), 499–507. https://doi.org/10.3390/forensicsci4040033.

Milanković, V., Tasić, T., Pašti, I.A., Lazarević-Pašti, T., 2024. MIP-based optical sensors: exploring principles and applications as artificial antibodies in disease detection and monitoring. In: Patra, S., Shukla, S.K., Sillanpää, M. (Eds.), Molecularly Imprinted Polymers: Path to Artificial Antibodies. Springer Nature Singapore, Singapore, pp. 273–297.

Moradian-Oldak, J., George, A., 2021. Biomineralization of Enamel and Dentin mediated by matrix proteins. J. Dent. Res. 100 (10), 1020–1029. https://doi.org/10.1177/00220345211018405.

Rathsam, C., Farahani, R.M., Hains, P.G., Valova, V.A., Charadram, N., Zoellner, H., Swain, M., Hunter, N., 2018. Characterization of inter-crystallite peptides in human enamel rods reveals contribution by the Y allele of amelogenin. J. Struct. Biol. 204 (1), 26–37. https://doi.org/10.1016/j.jsb.2018.06.006.

Sestaioni, D., Giurlani, W., Ciacci, G., Camagni, V., Palladino, P., Barucci, A., Scarano, S., 2024. Sustainable and effective reconditioning of SPR gold chips functionalized with molecularly imprinted polynorepinephrine. Anal. Chim. Acta 1321. https://doi.org/10.1016/j.aca.2024.343037.

Sestaioni, D., Ciacci, G., Barucci, A., Palladino, P., Scarano, S., 2025. Rational design of peptides for epitope imprinting of polynorepinephrine: a plasmonic and machine learning integrated approach. Biosens. Bioelectron. X, 100638. https://doi.org/10.1016/j.biosx.2025.100638.

Shaw, W.J., Tarasevich, B.J., Buchko, G.W., Arachchige, R.M.J., Burton, S.D., 2020. Controls of nature: secondary, tertiary, and quaternary structure of the enamel protein amelogenin in solution and on hydroxyapatite. J. Struct. Biol. 212, 3. https://doi.org/10.1016/j.jsb.2020.107630.

Shemirani, R., Le, M.H., Nakano, Y., 2023. Mutations causing X-Linked amelogenesis imperfecta alter miRNA Formation from Amelogenin Exon4. J. Dent. Res. 102 (11), 1210–1219. https://doi.org/10.1177/00220345231180572.

Stewart, N.A., Gerlach, R.F., Gowland, R.L., Gron, K.J., Montgomery, J., 2017. Sex determination of human remains from peptides in tooth enamel. Proc. Natl. Acad. Sci. U. S. A. 114 (52), 13649–13654. https://doi.org/10.1073/pnas.1714926115.

Torrini, F., Caponi, L., Bertolini, A., Palladino, P., Cipolli, F., Saba, A., Paolicchi, A., Scarano, S., Minunni, M., 2022a. A biomimetic enzyme-linked immunosorbent assay (BELISA) for the analysis of gonadorelin by using molecularly imprinted polymer-coated microplates. Anal. Bioanal. Chem. 414 (18), 5423–5434. https://doi.org/10.1007/s00216-021-03867-7.

Torrini, F., Battaglia, F., Palladino, P., Scarano, S., Minunni, M., 2022b. Imprinted biopolymers as green abiotic route in immunoglobulin affinity plasmonic sensing. Biosens. Bioelectron. 217. https://doi.org/10.1016/j.bios.2022.114706.

Torrini, F., Battaglia, F., Sestaioni, D., Palladino, P., Scarano, S., Minunni, M., 2023. Monoclonal antibodies (mAbs) optical detection by coupling innovative imprinted biopolymers and magnetic beads: the case of therapeutic mAb anti-myostatin detection. Sensor. Actuator. B Chem. 383. https://doi.org/10.1016/j.snb.2023.133586.

Torrini, F., Ferraro, G., Fratini, E., Palladino, P., Scarano, S., Minunni, M., 2024. Toward nano-sized imprinted norepinephrine-derived biopolymer as artificial receptors for detecting IgG1 by surface plasmon resonance. Biosens. Bioelectron. 252, 116–133. https://doi.org/10.1016/j.bios.2024.116133.

Veis, A., 2003. Amelogenin gene splice products: potential signaling molecules. CMLS Cell. Mol. Life Sci. 60, 38–55. https://doi.org/10.1007/s000180300003.

Ventisette, S., Ferruzzi, T., Sestaioni, D., Palladino, P., Minunni, M., Scarano, S., 2025. An antibody-free bio-layer interferometry biosensor for immunoglobulin G1 detection in human serum by using molecularly imprinted polynorepinephrine. Biosens. Bioelectron. 271. https://doi.org/10.1016/j.bios.2024.117095.

Wang, X., Xing, Z., Zhang, X., Zhu, L., Diekwisch, T.G.H., 2013. Alternative splicing of the amelogenin gene in a caudate amphibian, Plethodon cinereus. PLoS One 8, 6. https://doi.org/10.1371/journal.pone.0068965.

Wang, S., Zhang, L., Zeng, J., Hu, X., Wang, X., Yu, L., Wang, D., Cheng, L., Ahmed, R., Romanovski, V., Li, P., Zhang, Z., 2023. Multi-templates molecularly imprinted polymers for simultaneous recognition of multiple targets: from academy to application. TrAC, Trends Anal. Chem. 166, 117173. https://doi.org/10.1016/j.trac.2023.117173.

Zakaraia, S., Almohareb, M., Zaid, K., Doumani, M., Seirawan, M.Y., 2018. Amelogenin is a potential biomarker for the aggressiveness in odontogenic tumors. Asian Pac. J. Cancer Prev. APJCP : APJCP. 19 (5), 1375–1379. https://doi.org/10.22034/APJCP.2018.19.5.1375.